

BERENICE CLIFTON-GARCÍA<sup>1</sup>  
JUAN VILLAFANA-ROJAS<sup>2</sup>  
ORFIL GONZÁLEZ-REYNOSO<sup>3</sup>  
JORGE RAMON ROBLEDOR-ORTIZ<sup>1</sup>  
RICARDO MANRÍQUEZ-GONZÁLEZ<sup>1</sup>  
PORFIRIO GUTIÉRREZ-GONZÁLEZ<sup>4</sup>  
YOLANDA GONZÁLEZ-GARCÍA<sup>1</sup>

<sup>1</sup>Departamento de Madera, Celulosa y Papel, Centro Universitario de Ciencias Exactas e Ingenierías, Universidad de Guadalajara. Guadalajara, México

<sup>2</sup>Departamento de Biotecnológicas y Ambientales, Universidad Autónoma de Guadalajara, México

<sup>3</sup>Departamento de Ingeniería Química, Centro Universitario de Ciencias Exactas e Ingenierías, Universidad de Guadalajara. Guadalajara, México

<sup>4</sup>Departamento de Matemáticas, Centro Universitario de Ciencias Exactas e Ingenierías, Universidad de Guadalajara. Guadalajara, México

SCIENTIFIC PAPER

UDC 628.35:66:633.15

## USE OF AN INTERNAL LOOP AIRLIFT BIOREACTOR TO PRODUCE POLYHYDROXYALKANOATES BY *Stenotrophomonas rhizophila*

### Article Highlights

- First report on *Stenotrophomonas rhizophila* culture using cheap molasses to produce PHB
- High biomass and PHA yields were reached using an easy-to-construct airlift bioreactor
- A feeding strategy based on replenishing the liquid loss resulted in high polymer accumulation

### Abstract

*Airlift-type bioreactors present advantages over conventional systems such as efficient mass transfer, simplicity of construction, and low energy consumption. Thus, they are a good alternative for the production of polyhydroxyalkanoates (PHAs) nevertheless, their use for that purpose has been barely studied. This work addresses the design, construction, and hydrodynamic characterization of a 2.4 L internal loop airlift bioreactor, evaluating the effect of the airflow, liquid volume, and disperser position, on the interfacial area and the mixing time. Then, it was used for the fed-batch production of PHB by *Stenotrophomonas rhizophila* from sugar cane molasses. It was found that the conditions to increase the interfacial area and minimize the mixing time were: airflow of 1.5 vvm, liquid volume of 2400 mL, and disperser position of 5 mm (distance between the air disperser and the drag tube). Under that configuration, the maximum biomass concentration, PHB production, and PHB accumulation achieved (54 h of culture) were 65.4 g/L, 39.9 g/L, and 60.2 % (g of PHB/100 g dry biomass), respectively. The polymer was poly-3-hydroxybutyrate, with a melting temperature of 170°C, crystallinity of 56.4 %, and a Mw of 735 kDa.*

*Keywords:* airlift bioreactor; molasses; polyhydroxyalkanoates; *Stenotrophomonas rhizophila*.

Polyhydroxyalkanoates (PHAs) are microbial bioplastics accumulated as intracellular granules by different microbial species under conditions of nutritio-

nal stress caused by an excess of a carbon source accompanied by a deficit of other nutrient (nitrogen, phosphorus, magnesium, among others) [1–2]. This kind of biopolyester can behave as thermoplastics or elastomers (depending on their chemical structure) with physical, chemical, and mechanical properties similar to those of petroleum-based plastics such as polypropylene [1–2]. PHAs, unlike plastics of petrochemical origin, are obtained from renewable carbon sources and are biodegradable, which is a great advantage. In addition, they are biocompatible and can be used in the biomedical field. The PHAs' production process has been focused on the use of stirred tank

Correspondence: Y.González-García, Departamento de Madera, Celulosa y Papel, Centro Universitario de Ciencias Exactas e Ingenierías, Universidad de Guadalajara. Blvd. Gral. Marcelino García Barragán 1421, Olímpica, 44430 Guadalajara, Jal.  
E-mail: yolanda.ggarcia@academicos.udg.mx  
Paper received: 19 August, 2023  
Paper revised: 16 March, 2024  
Paper accepted: 17 April, 2024

<https://doi.org/10.2298/CICEQ230819014C>

bioreactors. The airlift-type bioreactor has been less used for this purpose, though it is an interesting alternative as demonstrated by some reports, in which biomass production and polymer accumulation showed encouraging data [3–6]. Airlift reactors promote pneumatical agitation with flows in the defined cycle. Among their advantages are the absence of moving parts, low shear stresses, low energy consumption, good mixing, and efficient mass transfer. Moreover, they are easy to manufacture and scale up. The agitation and mixing in this type of reactor occurs using an internal or external loop. As for the internal loop airlift, the reactor consists of two concentric tubes, with an ascent zone of the liquid with gas, and a descent zone where the liquid is relatively gas-free. The enhanced performance of an airlift bioreactor for aerobic fermentation processes depends on its hydrodynamic behavior. This analysis is based on the evaluation of dynamic parameters such as the mixing time and the gas-liquid interfacial area (calculated from the bubble size and the gas retention value). The operation variables most important for the bioreactor performance include the disperser position (the distance on the *y-axis* between the air disperser and the drag tube), airflow, and volume of the liquid [7–10].

Besides the use of low-energy consuming bioreactors, such as the airlift-type for producing PHAs, another important fermentation strategy to achieve a competitive process, is based on the formulation of culture media from inexpensive carbon sources, such as sugarcane molasses.

It is a sugar-rich viscous liquid generated after the sugar extraction from the sugarcane. The main carbohydrate in molasses is sucrose, followed by some fructose and glucose. In addition, molasses contains minerals and vitamins in small concentrations [11]. They are generated in many tropical countries, where sugarcane is a major crop. In Mexico (2018), 51 sugarcane mills produced around 5.8 Mtons of sugar and 1.76 Mtons of molasses [12], so they are a promising, abundant, and available substrate for the cost-effective production of PHAs. This has been investigated using some bacteria such as *Pseudomonas fluorescens* A2a5, *Bacillus megaterium* ATCC6748, *Cupriavidus necator* DSM 545 [13], *Bacillus cereus* SS105, *Ralstonia eutropha* ATCC 17699 [14], *Pseudomonas corrugata*, *B. cereus* SPV [15], *B. subtilis* AMN1, mixed cultures [16], *B. megaterium* BA-019, *B. flexus* AZU-A2, *B. subtilis* BPP-19, and *Clostridium beijerinckii* ASU10 [17]. However, molasses might contain high concentrations of growth inhibitors (phenolic compounds, melanoidins, metal ions, etc.), so this substrate must be pretreated before fermentation to reduce the inhibitory effect it has

on many PHAs-producing bacteria [17–18]. Another issue about using molasses as a carbon source is that only a few PHA-producing bacteria can metabolize the sucrose contained in it. Thus, it is necessary to genetically modify such bacteria for them to express the gene that encodes for the enzyme  $\alpha$ -fructofuranosidase, which is responsible for the hydrolysis of sucrose (a critical step to metabolize this disaccharide) [18].

On the other hand, *Stenotrophomonas rhizophila* (a bacterium isolated by our group [19], used in the present research) has demonstrated the ability to assimilate sucrose (without requiring genetic modifications), and to grow in the presence of inhibitory compounds [20–22]. Therefore, it is expected to produce PHAs from molasses, without pretreatment.

Considering the above, the present research is focused on the hydrodynamic characterization of an internal loop airlift bioreactor and its use for cultivating *S. rhizophila* using molasses as a low-cost substrate. It is expected that by changing the operation variables previously mentioned, an appropriate configuration for increasing the interfacial area and decreasing mixing time will be attained, which would favor the growth and biopolymer by *S. rhizophila*.

## MATERIAL AND METHODS

### Airlift bioreactor design and construction

The stainless steel T304 airlift bioreactor built was an internal loop concentric tube type, designed to operate with a maximum working volume of 2.4 L. Its geometric ratios are 0.33 between the diameter of the drag tube and the diameter of the outer tube, 6.56 between the height and diameter of the outer tube, and 0.57 between the heights of the inner and outer tubes [23–25], as shown in Fig. 1. This design was conceived based on the recommended ratios for airlift reactors (less than 10 liters) found in the literature: 0.3, between the diameter of the drag tube and the diameter of the outer tube; 6, between the height and diameter of the outer tube; and 0.6, between the heights of the inner and outer tubes [24]. The versatility of the airlift reactor's design makes it flexible because the modification of the drag tube is simple. Despite the ratio differences (with respect to that reported in the literature), the functionality of the airlift bioreactor built was considered appropriate according to the results obtained from the hydrodynamic analysis. It is worth mentioning that stainless steel polished surfaces influence gas retention and liquid velocity, as they contribute to a better performance of the pneumatic transport for the phases inside the bioreactor [24–27]. The airflow necessary for the pneumatic transport was

provided by compressed air at 2 bar, sterilized through a 0.2  $\mu\text{m}$  pore size membrane filter. It was controlled with a rotameter varying from 0.5 to 1.5 vvm. The control of the temperature at 30 °C was achieved with a heating blanket. On the bioreactor top lid, a condenser was placed to reduce the amount of water lost due to evaporation during fermentation, while at the bioreactor base, there were two valves: one used to sample and another to discharge.

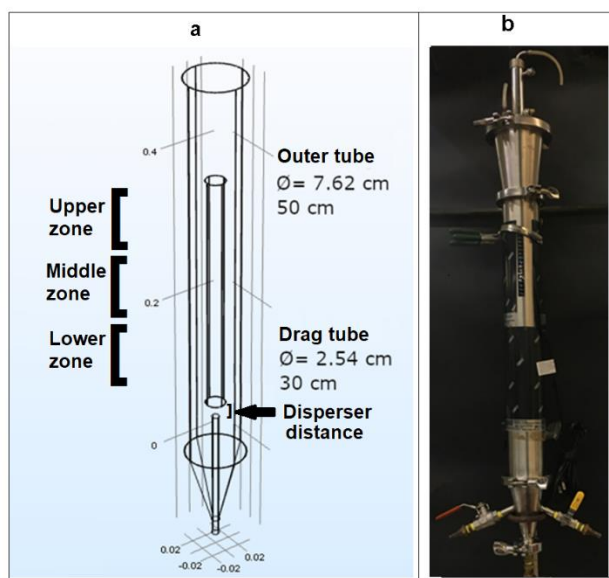


Figure 1. Airlift reactor. (a) design; (b) stainless steel.

### Hydrodynamic characterization

The hydrodynamic operation of the bioreactor was investigated according to a central composite design (CCD), which is a methodology used to explore the impact of independent variables (experimental factors) on response variables. Aeration flow, liquid volume, and disperser position, were the three independent variables studied, and their influence on two response variables was investigated: the interfacial area and mixing time. The CCD involves  $2^3$  factorial runs and a center point [28] (Table 1), resulting in nine experiments (Table 2). The confidence level used was 95%. This response surface optimization technique was applied to maximize the interfacial area and minimize the mixing time. The *STAGRAPHICS Centurion* program was used for data analysis.

Table 1. Factors and levels studied by the CCD experimental design.

Level	Airflow (vvm)	Liquid volume (mL)	Disperser position <sup>a</sup> (mm)
-1	0.5	2200	5
0	1	2300	10
1	1.5	2400	15

<sup>a</sup> Distance on the *y*-axis between the air disperser and the drag tube

The interfacial area Eq. (1) was calculated from Eq. (2), Eq. (3), and the equivalent bubble diameter [7]:

$$\text{Interfacial area: } A = \frac{6\varepsilon}{d(1-\varepsilon)} \quad (1)$$

$$\text{Retained volume: } \Delta V = V_{G+L} - V_L \quad (2)$$

$$\text{Volume expansion: } \varepsilon = \frac{\Delta V}{\Delta V + V_L} \quad (3)$$

where  $A$  is the Interfacial area ( $\text{cm}^2$ ),  $\varepsilon$  is the volume expansion,  $d$  is the bubble diameter (cm),  $\Delta V$  is the liquid volume expansion ( $\text{cm}^3$ ),  $V_L$  is the liquid volume ( $\text{cm}^3$ ), and  $V_{G+L}$  is the volume of gas and liquid ( $\text{cm}^3$ ).

The bubble size was determined by taking photographic shots of the bubbles (dividing the drag tube into three zones, Fig. 1). Later, the equivalent diameter was calculated using the Regionprops in the MatLab program, for the analysis, the photograph was transformed into grayscale and then the image was transformed to binary [7]. It is worth mentioning that transparent glass tubes were adapted to the airlift fermenter, instead of stainless-steel tubes, to visualize and measure the bubbles, as well as to determine the mixing time, as follows. A tracer pulse method was used: A pulse of tracer (1 mL of 0.1 M NaOH or 1 mL of 0.1 M HCl, depending on pH dissolution) was added to the bioreactor filled with distilled water with phenolphthalein as an indicator, at which point the time count was begun. The time was stopped when the color change was complete throughout the reactor.

### Molasses characterization

Sugar cane molasses was chosen as the carbon source, due to its high availability and low cost, it was provided by a local sugarcane mill. It was characterized for total sugars by the phenol-sulfuric method [29] and specific sugars by HPLC, using a Waters equipment with an IR 2914 detector and an HPX87P column (Biorad) at 85 °C. Water was used as the mobile phase with a flow rate of 0.6 mL/min. A molasses volume of 20  $\mu\text{L}$  (previously diluted 1:200) was filtered through a 0.45  $\mu\text{m}$  pore size membrane and analyzed. Total nitrogen and phosphate content was also determined (Kjeldahl and Vanadate-molybdate method, respectively) [30].

### Bacterial strain and inoculum preparation

The fermentation process to produce PHAs, using the airlift bioreactor, was carried out by *S. rhizophila*, a PHA-producing bacteria with the ability to metabolize sucrose [19]. The inoculum was prepared using the next culture medium (sucrose medium): sucrose, 20 g/L; NaCl, 2 g/L;  $\text{KH}_2\text{PO}_4$ , 2.25 g/L;  $(\text{NH}_4)_2\text{SO}_4$ , 10 g/L;  $\text{MgSO}_4 \cdot 7\text{H}_2\text{O}$ , 0.5 g/L;  $\text{CaCl}_2 \cdot \text{H}_2\text{O}$ , 0.02 g/L; yeast extract, 5 g/L; and peptone, 5 g/L. The pH was adjusted to 7. The inoculum was

prepared as follows: 6 to 10 isolated colonies growing in solid sucrose medium (agar, 16 g/L) were transferred to 10 mL of the same medium (120 mL Erlenmeyer flask) and incubated in a rotary shaker (24 h, 30 °C, and 150 rpm). Then, it was transferred to 230 mL of fresh medium (1L Erlenmeyer flask) and incubated as previously mentioned. Finally, this culture was used to inoculate the bioreactor.

### Fed-batch culture using the airlift bioreactor and molasses

The culture medium consisted of: molasses (20 g/L of total sugars); NaCl, 2 g/L; KH<sub>2</sub>PO<sub>4</sub>, 2.25 g/L; (NH<sub>4</sub>)<sub>2</sub>SO<sub>4</sub>, 10 g/L MgSO<sub>4</sub>·7H<sub>2</sub>O, 0.5 g/L; CaCl<sub>2</sub>·2H<sub>2</sub>O, 0.02 g/L; yeast extract, 5 g/L; peptone, 5 g/L. The amounts of major nutrients present in the diluted molasses were (in g/L) nitrogen 0.21 and phosphorus 0.01. The pH was adjusted to 7. A volume of 2200 mL of molasses medium was sterilized and aseptically added to the airlift bioreactor (previously sterilized); then, 200 mL of inoculum was added. The working volume (2400 mL) was set according to the results from the hydrodynamic study, as well as the airflow (1.5 vvm), and the disperser position (5 mm). The air was filtered using a Midistart 2000 sterile filter (0.20 µm PTFE, Sartorius); temperature and pH were maintained at 30 °C and 7, respectively.

Considering that a volume of 240 mL/day was lost (due to water evaporation and sampling) and that a nutrient imbalance condition was needed for PHA biosynthesis, a feeding strategy for gradually reaching a high C:N ratio, and simultaneously compensating the water loss was implemented (maintaining a constant volume). For that purpose, pulses of 120 mL of concentrated molasses (200 g/L), without any other culture medium's component, were added every 12 h. Five samples per day (20 mL each) were withdrawn and analyzed to determine: total sugars, total biomass, polymer, and ammonium concentration.

### Quantification of fermentation products and substrates

The determination of total carbohydrates was performed using the phenol-sulfuric method, and the specific sugars by HPLC as previously described.

The ammonium concentration was measured with an ammonium electrode (Cole-Parmer, 27504), and then used to calculate the C:N ratio in the culture medium.

For biomass quantification (denominated as total biomass), the samples were centrifuged for 30 min at 2200 *g*, then, the biomass pellet was washed with a physiological solution and centrifuged again. The washed biomass was freeze-dried (Labconco) and

weighed. The biomass resulting after PHB extraction was also weighed and represents the catalytic biomass (denominated as residual biomass in the present work).

For PHB quantification, the freeze-dried total biomass was suspended in 96% ethanol, at a 1:5 ratio (w/v), with agitation for 24 h. Subsequently, it was recovered by centrifugation and allowed to dry at room temperature for 24 h. The dry total biomass was resuspended in chloroform (1:5 w/v) in a glass flask with a magnetic stirrer (24 h). After that, the residual biomass was removed by filtration, and the chloroform was evaporated until a PHB film was formed and weighed (this step was performed twice). Finally, the remaining PHA inside the cells was determined by the crotonic acid method [31].

The biomass production data along the culture was fitted to a modified Gompertz equation (Eq. 4) to determine the kinetic parameters, using the Nonlinear Least Squares method to calculate the curve in MatLab [32].

$$X = L + C \cdot e^{-e^{-B(t-t_{max})}} \quad (4)$$

where  $X$  is the biomass (g/L).  $L$  is the lower asymptote value,  $C$  is the difference between the curve asymptotes,  $B$  is the relative growth rate,  $t$  is the time (h) and  $\mu_{max}$  is the maximum growth rate (1/h).

An exponential equation (Eq. 5) was used to predict the behavior of PHB production [33–34].

$$PHA = \frac{PHA_0 e^{\alpha t}}{1 - \left(\frac{PHA_0}{PHA_m}\right)(1 - e^{\alpha t})} \quad (5)$$

where  $PHA_0$  is the initial PHA (g/L),  $PHA_m$  is the maximum PHA (g/L),  $\alpha$  is the accumulation rate (1/h) and  $t$  is the time (h).

### Polymer characterization techniques

#### Nuclear Magnetic Resonance (NMR)

NMR proton (<sup>1</sup>H) and carbon (<sup>13</sup>C) spectra of the polymer were obtained using a benchtop Magritek Spinsolve 80 (80 MHz) spectrometer. The PHAs sample (5 mg) was dissolved in deuterated chloroform (0.7 mL) in a 5 mm diameter NMR tube and measured at room temperature.

#### Differential scanning calorimetry (DSC)

DSC analysis was performed by placing 5.67 mg of PHAs sample in aluminum capsules. The test was conducted at a heating rate of 10 °C/min from -20 to 182 °C under nitrogen flow using a Discovery DSCQ

200 equipment. From the thermograms, the peak of the melting temperature ( $T_m$ ) was obtained after a second melt of the sample, and the crystallinity ( $X_c$ ) was calculated Eq. (6):

$$X_c (\%) = \frac{\Delta H_{PHA} \cdot 100}{\Delta H_{ref}} \quad (6)$$

where  $X_c$  is the Crystallinity percentage (%),  $\Delta H_m$  is the experimental heat of fusion and  $\Delta H_{ref}$  is the heat of fusion (146 J/g) of fully crystalline PHA [35]. The cooling of the sample was obtained at the crystallization temperatures of the sample.

### Molecular weight

For molecular weight determination, the PHB sample was dissolved in chloroform (1.5 mg/mL) and then filtered (0.45  $\mu$ m). The equipment used was a Waters HPLC with an IR 2914 detector, using the GPC HR4 styragel column at 40°C. The mobile phase was NN-dimethylformamide (flow of 1 mL/min) and a sample volume of 20  $\mu$ L was injected. The calibration

curve was performed using polystyrene standards (Fluka 81437) with a molecular weight of 400 to 2,000,000 Da.

## RESULTS AND DISCUSSION

### Hydrodynamic characterization

In Table 2, the results from each experiment for the response variable, interfacial area, are presented. The airflow and the volume of liquid had a significant effect individually (Fig. S1a, Supplementary material): a greater interfacial area was found when setting the airflow or the volume of liquid at a high level (+1) which is a favorable response for the oxygen transference. On the other hand, the disperser distance does not have a significant effect by itself, but it does when interacting with the liquid volume (Fig. S1a): at disperser position (-1) combined with liquid volume (+1), the highest interfacial area is achieved. Thus, an increase in the airflow and liquid volume results in a rise in the interfacial area, which favors the oxygen transference, given the greater area for mass transference.

Table 2. Interfacial area and mixing time results according to the CCD experimental design (two replicates).

Experiment	Experimental Factors and levels			Response variables		Mixing time (s)	
	Airflow	Liquid volume	Disperser position	Interfacial area (mm <sup>2</sup> )		R1	R2
				R1	R2		
1	0	0	0	2489	2031	11.8	11.3
2	-1	-1	-1	697	705	15.9	16.1
3	1	-1	-1	3363	3650	8.1	7.8
4	-1	1	-1	1174	1301	11.2	11.2
5	1	1	-1	4506	4073	5.4	5.2
6	-1	-1	1	1001	975	15.4	17.4
7	1	-1	1	4099	3963	8.8	12.2
8	-1	1	1	1198	1157	12.2	12.1
9	1	1	1	3706	3927	6.1	6.4

Eq. (7), is the multiple regression equation that relates the response variable, interfacial area ( $A$ ), to the three independent variables: flow ( $F$ ), volume ( $V_L$ ), and disperser distance ( $D_d$ ). The lack of fit test for this equation confirms a linear association between the independent and response variables

$$A = 2474 + 1472F + 173.8V_L + 64.84D_d - 7.681FV_L + 8.045D_d - 156.0V_LD_d - 69.15FV_LD_d \quad (7)$$

where  $A$  is the Interfacial area (cm<sup>2</sup>),  $F$  is the airflow (volume of air per volume of liquid per minute (vvm),  $V_L$  is the liquid volume (cm<sup>3</sup>), and  $D_d$  is the disperser distance (mm).

Thus, it was found that, with the values of airflow (+1), volume of liquid (+1), and disperser position (-1), an area value of 4266 mm<sup>2</sup> was achieved. The main effect was attributed to the airflow (Fig. S1a). A similar result was reported by García-Albuín *et al.* [7]: an

increase in the airflow increased the interfacial area.

Since the interfacial area (Eq.1) depends on the retained volume (Eq. 2) and the bubble size, those were analyzed. As for the retained volume behavior (Fig. 2), it is directly proportional to the airflow [26–27, 36–37]: the experiments in which the airflow used was at the low level (-1) (two, four, six and eight) presented a lower retained volume than the experiments where the airflow was set at the high level (+1) (three, five, seven and nine). Meanwhile, in experiment one, the retained volume was an intermediate value since the airflow was set at the center point (0).

Regarding the bubble size, pictures were taken in the different reactor zones (lower, middle, and upper) (Fig. 1a). A change in the size of the bubbles as they ascended the drag tube was observed, it increased in the upper zone due to coalescence. The distribution of the equivalent diameters of the bubbles in each

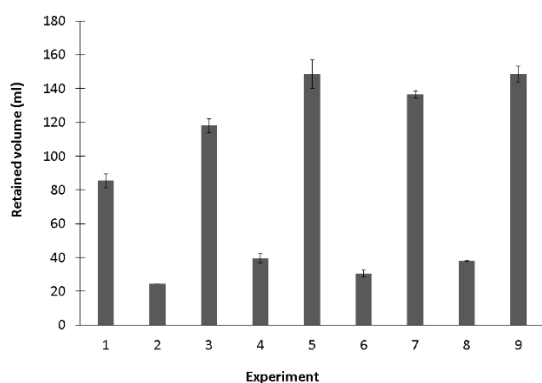


Figure 2. Behavior of the volume of retained air in each experiment (Table 2).

experiment is shown in Fig. 3. The bubble size distribution was more uniform between the different levels of the response factors, compared to those obtained by García-Abuín *et al.* [7] reporting bubble diameters of 6.2 and 9.5 mm (with airflows of 0.07 and 0.17 vvm), in 3.5 L airlift reactor (gas flows of 15 L/h and 36 L/h, respectively). The difference in the bubble diameter between the three zones is significant compared to the variation between the replicates of the different experiments.

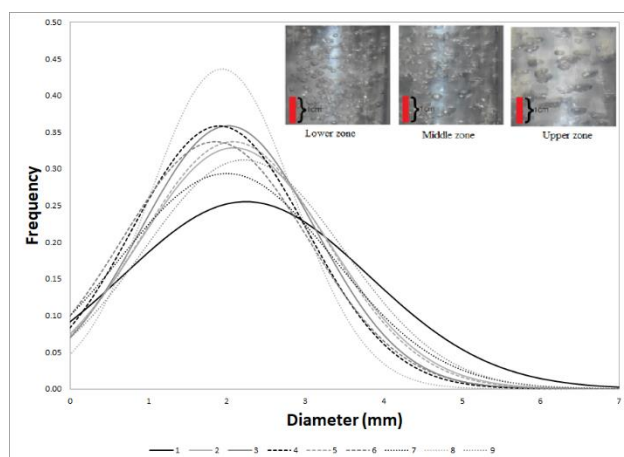


Figure 3. Bubble size distribution resulted in each experiment (Table 2).

Concerning the other response variable studied, mixing time, the results obtained from each experiment are shown in Table 2. The three independent variables tested individually (aeration flow, liquid volume, and disperser position) have a significant effect on this variable (Fig. S1b). The airflow is the factor that exerted the main influence (Fig. S1b), although liquid volume and disperser distance are also important for achieving a homogeneous system in the shortest time (Fig. S1b). Increasing the airflow (+1) results in improved

homogeneity, conversely, using a larger liquid volume (+1) decreases the mixing time within the tested range. About the disperser position, better mixing is favored when it is closer to the drag tube (-1), indicating that positioning the disperser close to the inlet of the drag tube is more efficient. The interaction between the independent variables on the mixing time was not significant (Fig. S1b).

Eq. (8), is the multiple regression equation that relates the three independent variables: flow ( $F$ ), volume ( $V_L$ ), and disperser distance ( $D_d$ ), to the response variable, mixing time ( $t_m$ ). The lack-of-fit test for this equation confirmed a linear relationship between the independent and response variables.

$$t_m = 10.8 - 3.22F - 1.99V_L + 0.603D_d + 0.264FV_L + 0.257FD_d - 0.137V_LD_d - 0.266FV_LD_d + 2474 + 1472F + 173.8V_L + 64.84D_d - 7.681FV_L + 8.045D_d - 156.0V_LD_d - 69.15FV_LD_d \quad (8)$$

where  $t_m$  is the mixing time (s),  $F$  is the airflow (volume of air per volume of liquid per minute (vvm)),  $V_L$  is the liquid volume ( $\text{cm}^3$ ), and  $D_d$  is the disperser distance (mm).

The faster mixing time (5.4 s) occurred in the next variables configuration: airflow (+1) 1.5 vvm, liquid volume (+1) 2400 mL, and distance between the disperser and the drag tube (-1) 5 mm. On the other hand, the slowest mixing time (16.4 s) was obtained in the following combination: airflow 0.5 vvm, liquid volume 2200 mL, and disperser position 15 mm (Table 2). The best results for both response variables, the interfacial area and mixing time, were obtained with high airflow (+1), corresponding to experiments three, five, seven, and nine (Table 2).

The optimization (according to the statistical analysis, within the ranges studied) to increase the interfacial area and decrease the mixing time resulted in the following conditions: airflow of 1.5 vvm (3.6 L/min); liquid volume of 2400 mL; and disperser distance of 5 mm (Fig. S2).

### Chemical composition of molasses

The characterization of molasses (raw, not diluted) shows a total sugar content of 456.3 g/L (sucrose, 91%; fructose, 6%; and glucose, 3%); and the total nitrogen and phosphorous concentrations were (g/L): 4.8 and 0.28, respectively. Those values are within the range reported for sugarcane molasses: total sugars 200–500 g/L, nitrogen 2.5–8.5, and phosphorus 0.25–1.8 [38–41]. It was important to point out that molasses was diluted to reach a final concentration of 20 g/L of total sugars and then used as a base for the culture medium. Therefore, the

amounts of phosphorous and nitrogen in such molasses were (g/L) 0.21 and 0.01, which are low values to be considered as an interference for the PHB accumulation process.

### Fed-batch culture using the airlift bioreactor and molasses

In Table 3, the results from the fermentation, including major kinetic parameters are shown, as well as those from other similar studies, using other strains, carbon sources, and bioreactor types. Fig. 4a shows the total biomass production and the PHB

accumulation kinetics of *S. rhizophila* growing in the airlift bioreactor with molasses as a carbon source. As described in the materials and methods section, molasses were fed in pulses every 12 h, the added also compensated for the water lost due to evaporation caused by aeration, maintaining a constant volume within the reactor. A modified Gompertz equation (Eq. 4) was used to fit the biomass production experimental data (Fig. 4c), obtaining an R-square value of 98.3%. For PHB accumulation, a fitting to an exponential equation (Eq. 5) was performed (Fig. 4d), with an R-square value of 96.1%.

Table 3. PHAs production from sugarcane molasses or sucrose, in airlift and stirred tank bioreactors.

Bioreactor Type/Volume (L)	Carbon source	Strain	Total biomass (g/L)	PHAs (g/L)	PHAs (%)	Productivity (PHAg/Lh)	$Y_{x/s}$ (g/g)	$\mu_{max}$ (1/h)	Reference
Airlift	2.4 Molasses	<i>Stenotrophomonas rhizophila</i>	65.4	39.3	60	0.73	0.39	0.27	This work
	7 Starch hydrolyzate	<i>Halomonas boliviensis</i>	9.2	5.2	56	0.21	0.43	0.45	[5]
	10 Glucose+fructose	<i>Ralstonia eutropha</i>	4.1	1.5	37	0.6	-	0.32	[6]
	4 Sucrose	<i>Azohydromonas australica</i>	10.8	7.8	73	0.21	0.43	0.45	[3]
	8 Sucrose	<i>Burkholderia sacchari</i>	150.0	63.0	42	1.07	0.4	0.4	[4]
Stirred tank	7 Sucrose	<i>Azohydromonas australica</i>	27.9	20.6	73	0.3	0.28	-	[42]
	3 Sucrose	<i>Burkholderia sacchari</i>	36.5	20.4	56	1.29	0.18	0.23	[43]
	- Sucrose	<i>Azohydromonas lata</i>	142.0	68.4	50	3.97	-	-	[44]
	3 Sucrose	<i>Burkholderia sacchari</i>	74.6	53.7	72	1.29	0.38	0.18	[43]
	5 Molasses	<i>Pseudomonas fluorescens</i>	32.0	22.4	70	0.23	-	-	[45]
	3 Molasses	<i>Azohydromonas lata</i>	-	5.7	68	0.16	-	-	[46]
	10 Molasses	<i>Bacillus megaterium</i>	32.5	8.8	26.9	0.73	0.69	0.29	[47]

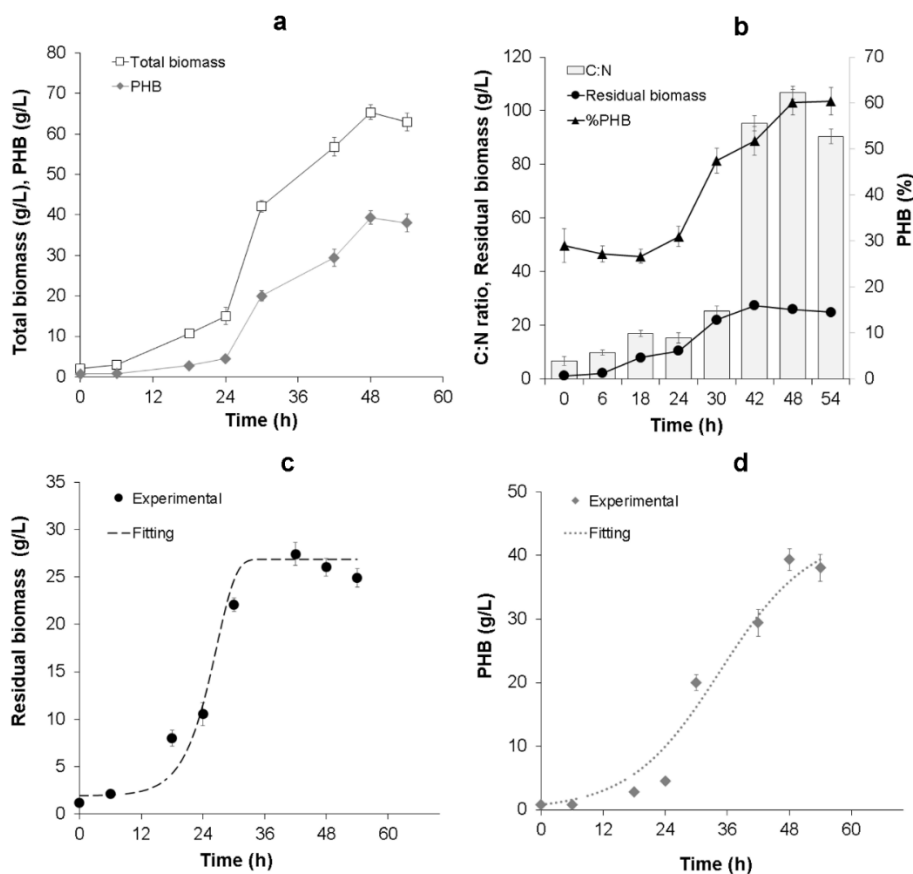


Figure 4. Kinetic profile for biomass production and PHA accumulation by *S. rhizophila* growing in the airlift bioreactor (fed-batch).

It is observed (Fig. 4a) that during the first 24 h, bacterial growth is slow. Then, the exponential growth phase begins and continues until 30 h of culture. After this point, bacterial growth slows down because of the progressive depletion of nutrients other than the carbon source, as only concentrated molasses (without any other nutrient) was periodically fed into the bioreactor, as pulses. From 30 h of culture, the increment in total biomass observed is mostly due to the increment in PHB accumulation within the cell (Fig. 4a). This is more clearly observed in Fig. 4b, where the residual biomass concentration (catalytic biomass) remains almost constant from the 30 h to 54 h of culture, while the percentage of PHB rises, from 31 (at 24 h) to 60.2. It is interesting to point out that *S. rhizophila* synthesizes the polymer before a low nitrogen concentration in the culture medium occurs (0–24 h) (Fig. 4b), though the accumulation increased considerably upon nitrogen limitation (high C:N due to the feeding/consumption of molasses and the continuous ammonia intake). The behavior observed in Fig. 4b is very similar to that presented by *A. latus* DSM1123: a high polymer content at nitrogen-sufficient conditions (around 50%), and an even higher accumulation of (90%) under nitrogen-limiting conditions [48]. Related to the above, Kiselev *et. al* [49] (using hydrolyzed sugar beet molasses to produce PHB by *C. necator*) reported that the amount of polymer accumulated before nitrogen depletion was around 30% (24 h), which is similar to our results. Likewise, after that point the C:N ratio raised, triggering a higher intracellular PHB content (75%) [49]. In this regard, studies on the effect of the C:N ratio on the PHAs accumulation by different bacteria, confirmed that the polymer biosynthesis is stimulated when the C:N ratio rises: *A. australica*, from 41.6 to 60 (PHAs 73%) using sucrose [3]; *Azotobacter chroococcum* 6B, from 68.9 to 137.7 (PHB 63.5%) using glucose [50]; and *Cupriavidus necator*, from 36.1 to 360 (PHAs 80%) on the use of rice hydrolysates [51]. In Fig. 4b, it is observed that the C:N ratio changed from 7:1 (initial condition) to 107:1 (48 h) due to nitrogen source consumption in combination with the carbon source accumulation (which is a regular feature of PHAs production in fed-batch culture). For *S. rhizophila*, the PHB accumulation increased at C:N ratios around 100.

The maximum total biomass concentration, PHB production, and PHB accumulation were: 65.4 g/L, 39.3 g/L, and 60.2 (g PHB/100 g dry biomass). Compared to the same bacterium, the only result reported is from flask cultures: 1.7 g/L of biomass and a PHB content of 13.7% [19]. The results from the present research are higher than those reported for other strains cultivated in similar culture systems (airlift bioreactor, fed-batch culture), such as *Halomonas*

*boliviensis*, *Ralstonia eutropha* and *Azodyromonas australica* [3, 5–6], as observed in Table 3. On the other hand, are lower than those presented by *Burkoderia sacchari* growing from sucrose, in an airlift bioreactor [4] (Table 3). However, it is important to remark that in that research; an aeration rate of 12.6 vvm was used, which is notably higher (8 times) than that used in the present research (1.5 vvm). *S. rhizophila* presented a  $\mu_{max}$  of 0.27/h, a total biomass and PHB yields on substrate ( $Y_{X/S}$  and  $Y_{P/S}$ ) of 0.39 g/g, and 0.23 g/g, respectively. Those values are within the range reported for other PHAs-producing strains cultivated in airlift bioreactors, such as *R. eutropha* and *A. australica* (Table 3) [3,6], yet it has to be mentioned that it was achieved at a low aeration rate. The PHB accumulation rate was 0.1151/h, and the  $PHAs_m$  (the maximum PHB accumulation expected) was 43.64 g/L, according to the results from the exponential equation used to fit the experimental data (Eq. 5).

As for the use of sugar cane molasses or sucrose as the carbon source to produce PHAs by other bacteria (but cultured in stirred tank reactors) the ranges of biomass production and polymer accumulation are variable (Table 3), yet the production of PHB by *S. rhizophila* from molasses is in the higher range, with the advantages of using a low-energy consuming airlift bioreactor.

### Polymer characterization

In Fig. 5a, it is shown the  $^1H$  NMR spectrum of the polymer obtained (see chemical structure). Here, PHB repeat unit presence is observed by its classical hydrogen signals pattern of CH at 5.5, CH<sub>2</sub> at 2.5 and CH<sub>3</sub> at 1.3 ppm (in the corresponding integration ratio of 1:2:3). Although CH and CH<sub>3</sub> signals showed the expected multiplicity as sextet and doublet, signal of CH<sub>2</sub> did not split as a doublet of quartet (as reported) [52–55] due to the low magnetic field (80 MHz NMR spectrometer) used in the measurement. However, in this case, the important data already demonstrated the identity of the polymer produced: poly-3-hydroxybutyrate. This identity is also corroborated by four carbon signals shown in the  $^{13}C$  NMR spectrum of Fig. 5b. Here, the signal at 168 ppm corresponded to carbonyl carbon from the ester group (C1), and its aliphatic carbon backbone is demonstrated in the signals at 66 (C3), 39 (C2) and 18 ppm (C4) associated to methine, methylene, and methyl groups, respectively.

The results of melting temperature ( $T_m$ ) were 170 °C ( $\Delta H=82.3$  J/g) and the percentage of crystallinity ( $X_c$ ) was 56.4. The thermograms obtained were as those reported in other PHB production studies, indicating a similar thermal behavior. The

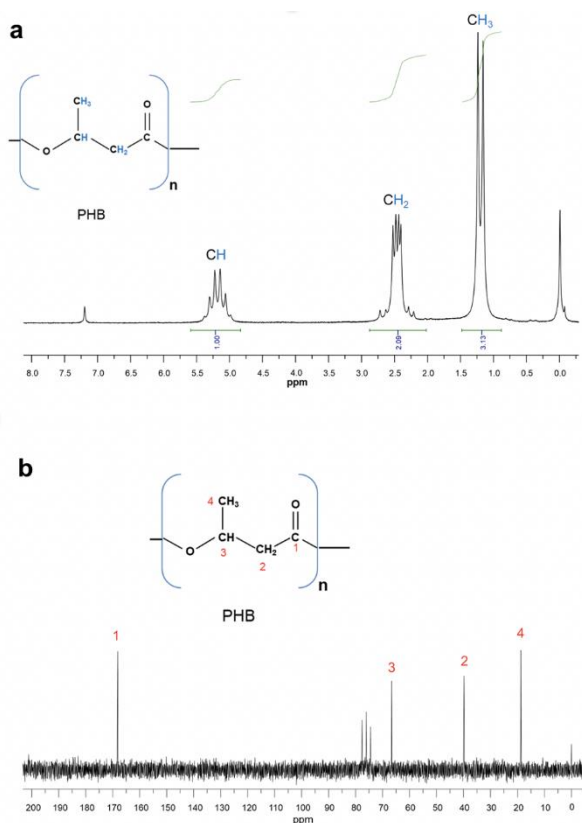


Figure 5. <sup>1</sup>H NMR (a) and <sup>13</sup>C NMR (b) spectra of the PHAs obtained.

values obtained match those reported for PHB. The  $T_m$  is from 164–180 °C and for crystallinity, the range is from 50% to 80% [34,56–58].

The number average molecular weight ( $M_n$ ), weight average molecular weight ( $M_w$ ), and the polydispersity index of the PHB produced by *S. rhizophila* were: 310 kDa, 735 kDa, and 2.37. This characteristic depends on several factors, such as the activity and type of PHAs synthetase present in the strain, the type and concentration of the carbon source used, and even the polymer extraction process and purification [59]. Thus, the molecular weight of PHAs produced by different strains under their specific culture conditions is variable. For example, PHAs produced by *Halomonas* sp. weigh 124 kDa (glycerol) in contrast to the 957 kDa of the polymer from *C. necator* DSM 545 (glycerol). Therefore, because the  $M_w$  of the polymer synthesized by *S. rhizophila* from molasses was 735 kDa, it is within the reported ranges previously mentioned. The molecular weight of PHAs is directly related to other mechanical and physical characteristics. Depending on their intended use, it will be their desirable molecular weight.

## CONCLUSION

The hydrodynamic characterization of the airlift

bioreactor allowed a configuration to minimize the mixing time and maximize the interfacial area. Under such conditions, using a low airflow, and a feeding strategy based on liquid loss compensation, *S. rhizophila* achieved a relevant biomass production with a high polymer accumulation. Thus, these results confirmed that the low-energy consuming airlift bioreactors are suitable for PHA production and that *S. rhizophila* is a promising bacterium to produce PHB from molasses. The next step is to evaluate its ability to produce copolymers. Further studies are necessary to enhance this process: the effect of increasing the molasses concentration; optimization of the culture medium and culture conditions (i.e. pH and temperature); the PHB accumulation under different nutrient-limiting conditions (i.e. phosphorous); and the implementation of other operation modes (i.e., perfusion). In addition, the modeling and simulation of the bioreactor, as well as the scale-up studies are also important aspects to consider.

## ACKNOWLEDGMENT

To CONACyT for the postdoctoral fellowship granted to Berenice Clifton-Garcia (839863) and COECYTJAL, for the financial support (project 8092-2019).

## NOMENCLATURE

$A$	Interfacial area (cm <sup>2</sup> )
$B$	Relative growth rate
$C$	Difference between the curve asymptotes
$Dd$	Disperser distance (mm)
$d$	Bubble diameter (cm)
$F$	Airflow (volume of air per volume of liquid per minute (vvm))
$L$	Lower asymptote value
$PHA_0$	PHA initial (g/L)
$PHA_m$	PHA maximum (g/L)
$t$	Time (h)
$t_m$	Mixing time (s)
$V_L$	Liquid volume (cm <sup>3</sup> )
$V_{(G+L)}$	Volume of gas and liquid (cm <sup>3</sup> )
$X$	Biomass (g/L)
$X_C$	Crystallinity percentage (%)
<i>Greek letters</i>	
$\alpha$	Accumulation rate (/h)
$\varepsilon$	Volume expansion (Holdup)
$\mu_{max}$	Maximum growth rate (/h)
$\Delta H_{PHA}$	Experimental fusion enthalpy (J/g)
$\Delta H_{ref}$	Reference melting enthalpy (146 J/g)
$\Delta V$	Liquid volume expansion (cm <sup>3</sup> )

## REFERENCES

- [1] Y. González García, J.C. Meza Contreras, O. González Reynoso, J.A. Córdova López, Rev. Int. de Contam. 29 (2013) 77–115. <https://www.scielo.org.mx/pdf/rica/v29n1/v29n1a7.pdf>.
- [2] T. Keshavarz, I. Roy, Curr. Opin. Microbiol. 13 (2010) 321–326. <https://doi.org/10.1016/j.mib.2010.02.006>.
- [3] G. Gahlawat, B. Sengupta, A.K. Srivastava, J. Ind.

- Microbiol. Biotechnol. 39 (2012) 1377–1384. <https://doi.org/10.1007/s10295-012-1138-5>.
- [4] J.G da C. Pradella, M.K Taciro, A.Y.P. Mateus, Bioresour. Technol. 101 (2010) 8355–8360. <https://doi.org/10.1016/j.biortech.2010.05.046>.
- [5] P. Rivera-Terceros, E. Tito-Claros, S. Torrico, S. Carballo, D. Van-Thuoc, D. Quillaguamán, J. of Biol. Res-Thessaloniki. 22 (2015) 8. <https://doi.org/10.1186/s40709-015-0031-6>.
- [6] L.Z. Tavares, E.S da Silva, J.G da C. Pradella, Biochem. Eng. J. 18 (2004) 21–31. [https://doi.org/10.1016/S1369-703X\(03\)00117-7](https://doi.org/10.1016/S1369-703X(03)00117-7).
- [7] A. García-Abuín, D. Gómez-Díaz, ACI. 1 (2010) 2 25–36. <https://api.semanticscholar.org/CorpusID:93351577> ISSN-e0718-8706.
- [8] G.B. Hurtado, A.M. Otálvaro, P.G. Duarte, Rev. Colomb. Biotecnol. 15 (2013) 106–114. <https://doi.org/10.15446/rev.colomb.biote.v15n2.41272>.
- [9] J.C. Merchuk, Can. J. Chem. Eng. 81 (2003) 324–337. <https://doi.org/10.1002/cjce.5450810301>.
- [10] G. Quijano, S. Revah, M. Gutiérrez-Rojas, L.B. Flores-Cotera, F. Thalasso, Process Biochem. 44 (2009) 619–624. <https://doi.org/10.1016/j.procbio.2009.01.015>.
- [11] L. Jamir, V. Kumar, J. Kaur, S. Kumar, H. Singh, H. Environ. Technol. Rev. 10 (2021) 1, 131–142. <https://doi.org/10.1080/21622515.2021.1892203>.
- [12] J. Aburto, E. Martínez-Hernández, Front. Energy Res. 8 (2021) 612647. <https://doi.org/10.3389/fenrg.2020.612647>.
- [13] K.Y. Sen, S. Baidurah, Curr. Opin. Green Sustainable Chem. 27 (2021) 100412. <https://doi.org/10.1016/j.cogsc.2020.100412>.
- [14] J. Wang, S. Liu, J. Huang, Z. Qu, Bioresour. Technol. 342 (2021) 126008. <https://doi.org/10.1016/j.biortech.2021.126008>.
- [15] A.T. Adeleye, C.K. Odoh, O.C. Enudi, O.O. Banjoko, O. O. Osiboye, E.T. Odediran, H. Louis, Process Biochem. 96 (2020) 174–193. <https://doi.org/10.1016/j.procbio.2020.05.032>.
- [16] S. Zhang, J. Wang, H. Jiang, Food Chem. 346 (2021) 128860. <https://doi.org/10.1016/j.foodchem.2020.128860>.
- [17] P. Marciniak, J. Mozejko-Ciesielska, Polymers 13 (2021) 11, 1731. <https://doi.org/10.3390/polym13111731>.
- [18] S. Y. Jo, Y.J. Sohn, S.Y. Park, J. Son, J.I. Yoo, K.A. Baritugo, S.J. Park, Korean J. Chem. Eng. 38 (2021) 7, 1452–1459. <https://doi.org/10.1007/s11814-021-0783-7>.
- [19] B. Clifton-García, O. González-Reynoso, J.R. Robledo-Ortiz, J. Villafañá-Rojas, Y. González-García, Lett. Appl. Microbiol. 70 (2020) 300–309. <https://doi.org/10.1111/lam.13272>.
- [20] J. Gao, S. Wu, Y. Liu, S. Wu, C. Jiang, X. Li, X. Zhuang, X. Environ. Pollut. 263 (2020) 114622. <https://doi.org/10.1016/j.envpol.2020.114622>.
- [21] S.P. Kumar, B.K. Manjunatha, Sci., Technol. Arts Res. J. 4 (2015) 3, 139–144. <https://www.ajol.info/index.php/star/article/view/142953>.
- [22] B.N. Sánchez-Pérez, A. Zenteno-Rojas, C.I. Rincón-Molina, V.M. Ruiz-Valdiviezo, F.A. Gutiérrez-Miceli, M. A., Vences-Guzmán, R. Rincón-Rosales, Water, Air, Soil Pollut. 231 (2020) 1–15. <https://doi.org/10.1007/s11270-020-04481-6>.
- [23] M. Moo-Young, Comprehensive Biotechnology, Academic Press, Burlington (2011), p. 199. <https://doi.org/10.1016/B978-0-08-088504-9.00095-7>.
- [24] E.R. Gouveia, C.O. Hokka, A.C. Badino-Jr, Braz. J. Chem. Eng. 20 (2003) 363–374. <https://doi.org/10.1590/S0104-66322003000400004>.
- [25] G.C. Noverón, (2009). [Thesis, Instituto Politécnico Nacional] <https://tesis.ipn.mx/bitstream/handle/123456789/23318/Nover%c3%b3n%20Nava%20Guillermo%20Cuarto.pdf?sequence=1&isAllowed=y>.
- [26] M. Blažej, M. Kiša, J. Markoš, Chem. Eng. Process. 43 (2004) 1519–1527. <https://doi.org/10.1016/j.cep.2004.02.003>.
- [27] J.C. Merchuk, M. Gluz, Encycl Bioprocess Technol. Eds M.C. Flickinger and S.W. Drew, New York (2002), p.320 <https://doi.org/10.1002/0471250589.ebt029>.
- [28] M. Mourabet, A. El Rhilassi, H. El Boujaady, M. Bennani-Ziatni, A. Taitai, Arabian J. Chem. 10 (2017) 2, 3292–3302. <https://doi.org/10.1016/j.arabjc.2013.12.028>.
- [29] M. DuBois, K.A. Gilles, J.K. Hamilton, P.A. Rebers, Anal. Chem. 28 (1956) 350–356. <https://doi.org/10.1021/ac60111a017>.
- [30] F.W. Gilcreas, Am J Public Health Nations Health. 56 (1966) 3, 387–388. <https://ajph.aphapublications.org/doi/pdf/10.2105/AJPH.56.3.387>.
- [31] M.P. Rajankar, S. Ravindranathan, P.R. Rajamohanam, A. Raghunathan, Biol. Methods Protoc. 3 (2018) 1. <https://doi.org/10.1093/biomethods/bpy007>.
- [32] C.M. Belda-Galbis, M.C. Pina-Pérez, J. Espinosa, A. Marco-Celdrán, A. Martínez, D. Rodrigo, Food Microbiol. 38 (2014) 56–61. <https://doi.org/10.1016/j.fm.2013.08.009>.
- [33] M. Mahmoudi, M.S. Baei, G.D. Najafpour, F. Tabandeh, H. Eisazadeh, Afr. J. Biotechnol. 9 (2010) 3151–3157. <https://doi.org/10.4314/ajb.v9i21>.
- [34] N. Moreno-Sarmiento, D. Malagón-Romero, J. Cortázar, A. Espinosa-Hernández, Univ. Scientiarum. 11 (2006) 41–48. <https://www.virtualpro.co/revista/universitas-scientiarum-vol-11-no-17>
- [35] E.V. Torres-Tello, J.R. Robledo-Ortiz, Y. González-García, A.A. Pérez-Fonseca, C.F. Jasso-Gastinel, E. Mendizábal, Ind. Crops Prod. 99 (2017) 117–125. <https://doi.org/10.1016/j.indcrop.2017.01.035>.
- [36] M. Mohajerani, M. Mehrvar, F. Ein-Mozaffari, Can. J. Chem. Eng. 90 (2012) 1612–1631. <https://doi.org/10.1002/cjce.20674>.
- [37] T. Zhang, C. Wei, C. Feng, J. Zhu, Bioresour. Technol. 104 (2012) 600–607. <https://doi.org/10.1016/j.biortech.2011.11.008>.
- [38] F. Veana, J.L. Martínez-Hernández, C.N. Aguilar, R. Rodríguez-Herrera, G. Michelena, Braz. J. Microbiol. 45 (2014) 373–377. <https://doi.org/10.1590/S1517-83822014000200002>.
- [39] K.P. Eliodório, G.C.D.G.E. Cunha, F.S.D.O. Lino, M.O.A. Sommer, A.K. Gombert, R. Giudici, T.O. Basso, Sci. Rep. 13 (2023) 1, 10567.

- <https://doi.org/10.1038/s41598-023-37618-8>.
- [40] M.S. Khatun, M. Hassanpour, S.I. Mussatto, M.D. Harrison, R.E. Speight, I.M. O'Hara, Z. Zhang, *Bioresour. Bioprocess* 8 (2021) 1–12. <https://doi.org/10.1186/s40643-021-00438-7>.
- [41] Y.D. N'Guessan, E.M. Bedikou, K.A. Otchoumou, C.I. Assemian, A.C. Ehon, *J. Sugarcane Res.* 11 (2023) 147–157. <https://doi.org/10.37580/JSR.2021.2.11.147-157>.
- [42] M. Koller, *Fermentation*, 4 (2018) 30. <https://doi.org/10.1007/s00449-013-0885-7>.
- [43] M. Miranda De Sousa Dias, M. Koller, D. Puppi, A. Morelli, F. Chiellini, G. Braunegg, *Bioengineering*, 4 (2017) 36. <https://doi.org/10.3390/bioengineering4020036>.
- [44] W. Blunt, Levin, N. Cicek, *Polymers*, 10 (2018) 1197. <https://doi.org/10.3390/polym10111197>.
- [45] L.R. Castilho, D.A. Mitchell, D.M. Freire, *Biores. Technol.* 100 (2009) 5996–6009. <https://doi.org/10.1016/j.biortech.2009.03.088>.
- [46] M. Zafar, S. Kumar, A.K. Dhiman, v J. *Ind. Microbiol. Biotechnol.*, 39 (2012) 987–1001. <https://doi.org/10.1007/s10295-012-1102-4>.
- [47] P. Kanjanachumpol, S. Kulpreecha, V. Tolieng, N. Thongchul, *Bioprocess Biosyst. Eng.* 36 (2013) 1463–74. <https://doi.org/10.1007/s00449-013-0885-7>.
- [48] F. Wang, S.Y. Lee, *Appl. Environ. Microbiol.* 63 (1997) 9 3703–3706. <https://doi.org/10.1128/aem.63.9.3703-3706.1997>.
- [49] E.G. Kiselev, A.V. Demidenko, N.O. Zhila, E.I. Shishatskaya, T.G. Volova, *Bioengineering* 9 (2022) 154. <https://doi.org/10.3390/bioengineering9040154>.
- [50] J.C. Quagliano, S.S. Miyazaki, *Appl. Microbiol. Biotechnol.* 48 (1997) 662–664. <https://doi.org/10.1007/s002530051112>.
- [51] J. Ahn, E.H. Jho, K. Nam, *Environ. Eng. Res.* 20 (2015) 246–253. <https://doi.org/10.4491/eer.2015.055>.
- [52] A. Bhattacharyya, A. Pramanik, S.K. Maji, S. Haldar, U.K. Mukhopadhyay, J. Mukherjee, *AMB Expr.* 2 (2012) 34. <https://doi.org/10.1186/2191-0855-2-34>.
- [53] C.K. Chang, H.M. Wang, J. Lan, *Polymers.* 10 (2018) 355. <https://doi.org/10.3390/polym10040355>.
- [54] W.H. Lee, C.Y. Loo, C.T. Nomura, K. Sudesh, *Bioresour. Technol.* 99 (2008) 6844–6851. <https://doi.org/10.1016/j.biortech.2008.01.051>.
- [55] R. Li, Y. Jiang, X. Wang, J. Yang, Y. Gao, X. Zi, X. Zhang, H. Gao, N. Hu, *Springer Plus.* 2 (2013) 335. <https://doi.org/10.1186/2193-1801-2-335>.
- [56] A.J. Dos Santos, L.V. Oliveira Dalla Valentina, A.A. Hidalgo Schulz, M.A. Tomaz Duarte, *Part I. Ing. Cienc.* 13 (2017) 269–298. <https://doi.org/10.17230/ingciencia.13.26.10>.
- [57] M. Koller, L. Marsalek, *Appl. Food Biotechnol.* 2 (2015) 3–15. <https://doi.org/10.22037/afb.v2i3.8271>.
- [58] H. Lu, S.A. Madbouly, J.A. Schrader, M.R. Kessler, D. Grewell, W.R. Graves, *RSC Adv.* 4 (2014) 39802–39808. <https://doi.org/10.1039/C4RA04455J>.
- [59] C. Insomphun, S. Kobayashi, T. Fujiki, K. Numata, *AMB Expr.* 6 (2016) 29. <https://doi.org/10.1186/s13568-016-0200-5>.

BERENICE CLIFTON-GARCÍA<sup>1</sup>  
JUAN VILLAFANA-ROJAS<sup>2</sup>  
ORFIL GONZÁLEZ-REYNOSO<sup>3</sup>  
JORGE RAMON ROBLEDO-  
ORTIZ<sup>1</sup>  
RICARDO MANRÍQUEZ-  
GONZÁLEZ<sup>1</sup>  
PORFIRIO GUTIÉRREZ-  
GONZÁLEZ<sup>4</sup>  
YOLANDA GONZÁLEZ-  
GARCÍA<sup>1</sup>

<sup>1</sup>Departamento de Madera, Celulosa  
y Papel, Centro Universitario de  
Ciencias Exactas e Ingenierías,  
Universidad de Guadalajara.  
Guadalajara, México

<sup>2</sup>Departamento de Biotecnológicas y  
Ambientales, Universidad Autónoma  
de Guadalajara, México

<sup>3</sup>Departamento de Ingeniería  
Química, Centro Universitario de  
Ciencias Exactas e Ingenierías,  
Universidad de Guadalajara.  
Guadalajara, México

<sup>4</sup>Departamento de  
Matemáticas, Centro  
Universitario de Ciencias  
Exactas e Ingenierías,  
Universidad de Guadalajara.  
Guadalajara, México

## UPOTREBA AIRLIFT BIOREAKTORA SA UNUTRAŠNJOM PETLJOM ZA PROIZVODNJU POLIHIDROKSIALKANOATA POMOĆU *Stenotrophomonas rhizophila*

*Bioreaktori tipa air-lifta imaju prednosti u odnosu na konvencionalne sisteme, kao što su efikasan prenos mase, jednostavnost konstrukcije i niska potrošnja energije. Zbog toga su oni dobra alternativa za proizvodnju polihidroksialkanoata (PHA), ali njihova upotreba u tu svrhu skoro da nije proučavana. Ovaj rad se bavi dizajnom, konstrukcijom i hidrodinamičkom karakterizacijom bioreaktora tipa air-lifta sa unutrašnjom petljom od 2,4 lL, procenjujući efekat protoka vazduha, zapremine tečnosti i položaja disperzatora na međufaznu površinu i vreme mešanja. Zatim je korišćen za proizvodnju PHB pomoću *Stenotrophomonas rhizophila* iz melase šećerne trske. Utvrđeno je da su uslovi za povećanje međufazne površine i minimiziranje vremena mešanja bili: protok vazduha od 1,5 vvm, zapremina tečnosti od 2400 ml i pozicija distributora od 5 mm (udaljenost između distributora vazduha i centralne cevi). U toj konfiguraciji, maksimalna koncentracija biomase, proizvodnja PHB i akumulacija PHB (54 h kulture) bili su 65,4 g/l, 39,9 g/l i 60,2 % (g PHB/100 g suve biomase), redom. Dobijeni polimer je poli-3-hidroksibutirat, sa tačkom topljenja od 170 °C, kristaliničnošću od 56,4 % i molekulskom masom od 735 kDa.*

*Ključne reči: airlift bioreaktor; melasa; polihidroksialkanoati; *Stenotrophomonas rhizophila*.*

NAUČNI RAD